Available online at www.sciencedirect.com
ScienceDirect
Thermochimica Acta 461 (2007) 72–81
thermochimica acta
www.elsevier.com/locate/tca

Evaluation of the calorimetric glass transition of glasses and glass ceramics with respect to structural relaxation and dimensional stability

Ulrich Fotheringham*, Rolf Müller, Klaus Erb, Andrea Baltes, Friedrich Siebers, Eveline Weiß, Roland Dudek

SCHOTT AG, Germany

Available online 28 June 2007

Abstract

Both for a borosilicate glass and a lithium–aluminium–silicate glass ceramic, it is found that quantitative predictions of the dimensional stability under thermal load are possible applying the semi-empirical Tool–Narayanaswamy–Moynihan model for structural relaxation, with the kinetic parameters obtained via DSC.

This adds two systems to the list of materials for which the correspondence of the relaxation kinetics of volume and enthalpy have been investigated.

Keywords: Glass transition; Tool–Narayanaswamy–Moynihan model; Dimensional stability

1. Introduction: calorimetric and dilatometric fingerprints of the glass transition in glasses and glass ceramics

In a crystal which is an ordered system with translational symmetry, the ensemble made up by any atom and its neighbours may be mapped onto the corresponding atoms of the unit cell. This means that there is essentially one configurational state (in simple crystals) or there are at least only few configurational states (such as in molecular crystals) in which an atom of one kind may be found. In a glass which is a disordered system without translational symmetry there are many different such configurational states [1]. (This must be the case because otherwise the material would be ordered.) As there is no reason for any atomic ensemble to be in one particular of these configurational states, the multitude of these configurational states gives rise to a corresponding number of degrees of freedom (Fig. 1).

These configurational degrees of freedom, in return, give rise to a characteristic feature of the glassy state, the calorimetric glass transition. As the energy levels of the different configurational states are not the same (any energetic degeneration of states would be very unlikely), the glass will change the average configurational energy level according to the environmental temperature. Consider the case of constant environmental temperature and pressure as well as the corresponding thermodynamic potential, i.e. Gibbs' free energy G:

$$G = E + PV - ST \tag{1}$$

P is the pressure, V the volume, S the entropy, and T is the temperature. To minimize Gibbs' free energy at higher temperatures, low energy and high energy configurations will be equally populated in order to increase the entropy. At lower temperatures, where the ST-term does not count so much, the low energy configurations will be preferred. For every temperature, there is an equilibrium distribution of atomic ensembles among the possible configurations.

If the glass is cooled down from high to low temperatures, this distribution will change accordingly thus lowering the average configurational energy. The redistribution of atomic ensembles among configurational states in order to reach equilibrium is called structural relaxation. (Note that minimization of Gibbs' free energy refers to the metastable supercooled liquid state which corresponds to a local minimum of G.)

The configurational changes involved, however, are kinetic processes with a time scale strongly depending on temperature.

* Corresponding author.
E-mail address: ulrich.fotheringham@schott.com (U. Fotheringham).

0040-6031/$ – see front matter © 2007 Elsevier B.V. All rights reserved.
doi:10.1016/j.tca.2007.06.007

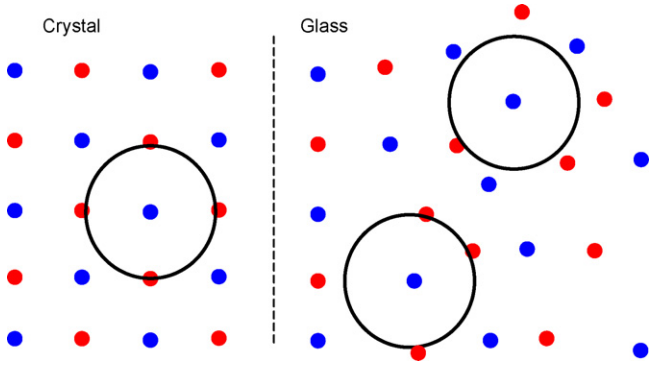

Fig. 1. Multitude of configurations for an atom and its environment in a glass as compared to a crystal.

This has two reasons. First, the transition of an atomic ensemble from one particular configurational state into another is hindered by a potential barrier and requires thermal activation. Second, the number of configurational states taking part in structural relaxation decreases with temperature (in other words: the configurational entropy is temperature dependent) which also makes the probability of a reconfiguration of an atomic ensemble decrease with decreasing temperature. Together, these two effects give rise to a temperature dependence of the structural relaxation time scale which is much stronger than the one of conventional thermal activation, as described by the Adam–Gibbs theory [1]. (Over a limited temperature range, one may describe this temperature dependence by an apparent thermal activation enthalpy; this apparent thermal activation enthalpy, however, is not temperature independent. It is the higher the lower the temperature range considered is.)

As a consequence, in a temperature range depending on the cooling rate, the time scale of the configurational changes will exceed the time scale of the cooling process (which is proportional to the inverse cooling rate; this is where the above dependence on the cooling rate comes from). This is the glass transition range in which the distribution of atomic ensembles among possible configurations freezes in [2].

If a glass is cooled down very slowly, this freezing-in will occur in a comparatively low temperature range or, characterising this temperature range by a single temperature, a comparatively low freezing-in temperature. The frozen-in distribution of atomic ensembles among configurational states will correspond to this temperature. If the same sample is heated up again rapidly thereafter, the thawing will occur at a comparatively high temperature. A significant redistribution of atomic ensembles among configurational states will follow because of the misfit of the frozen-in distribution to the temperature of thawing. The bigger the difference between the freezing-in temperature and the thawing temperature is, the bigger this misfit is.

Since the redistribution of atomic ensembles requires energy, one will find a strong peak in the differential scanning calorimeter curve [3]. This peak marks the calorimetric glass transition. At temperatures below the peak, the configurational degrees of freedom are frozen in and do not influence the specific heat which is then only determined by the vibrational degrees of freedom at these temperatures. At temperatures above the peak, the configurational degrees of freedom just come on top of the vibrational ones. This gives rise to the step of the specific heat which is one characteristic feature of the glass transition. The other characteristic feature is the above peak. The exact size of this peak depends on the misfit of the involved distributions of atomic ensembles which in return depends on the difference between cooling and reheating rate (Fig. 2).

The configurational changes above have some volumetric or dilatometric impact, too. If, for instance, a glass sample is equilibrated at a certain temperature (which means that the sample is held at this temperature long enough to allow the corresponding redistribution of atomic ensembles among the possible configurations) and then brought to another temperature, one will observe two effects involving dimensional changes. The first is the contribution of the regular thermal expansion. It is an instantaneous effect which is due to the change of medium atomic distances. The second is the contribution of the configurational changes and has their kinetics therefore. At high temperatures (i.e. at temperatures significantly above those where the calorimetric glass transition occurs for typical experimental conditions), it happens almost instantaneously and causes an additional contribution to the thermal expansion. At low temperatures, it is frozen in. In the temperature range of the glass transition, it is observed as delayed thermal expansion. Timescale and temperature of observation are linked (same as for the calorimetric glass transition the temperature range of which depends on the heating rate also).

This delayed thermal expansion is a crucial property of any glass that is exposed to a heat treatment at temperatures close to the glass transition range [4]. Such heat treatments occur, e.g. if a glass is coated with semiconductor layers as it happens during the fabrication of flat panel displays.

It is desirable to be able to make quantitative predictions of the dimensional stability during such a process. In the following, it will be shown for a glass and a glass ceramic that this is possible in a quick and easy way with a quantitative characterisation of the relaxation kinetics derived from differential

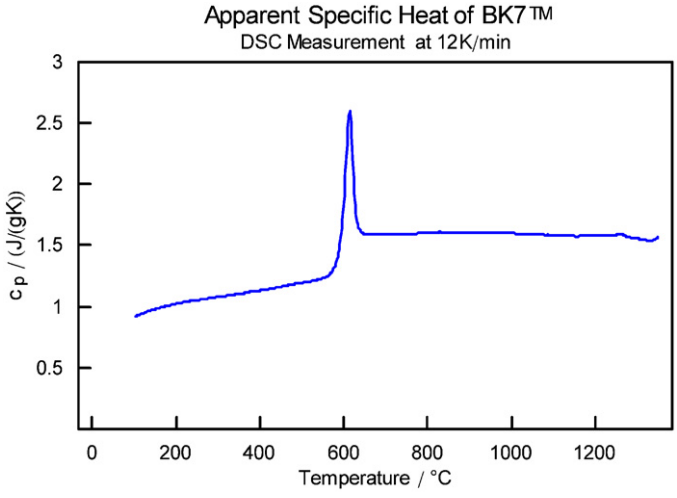

Fig. 2. Calorimetric glass transition of a borosilicate glass (BK7™ from SCHOTT AG) measured at 12 K/min.

scanning calorimeter measurements, if the latter are carried out in the appropriate way.

This is meant as a contribution to the discussion about the universality of the relaxation kinetics, in particular concerning enthalpy and specific volume (or density). There is literature both in favour of and against this idea. For glassy B_2O_3, differences between the relaxation kinetics of the enthalpy and the refractive index have been found [5]; as the refractive index depends on the density only as long as the modes of the atomic oscillators do not change (which can be monitored via the transmission curve), this indicates that enthalpy and density relaxation are not exactly the same for glassy B_2O_3. Some differences in kinetics have also been found for a polyetherimide [6].

There is also literature in support of the idea that enthalpy and specific volume should have the same relaxation kinetics, at least in a limited temperature range around the annealing point. See [7] for NIST SRM 710 standard soda-lime glass, [8] for As_2Se_3, As_2S_3, PS, PVA, PC, PMMA, PVC, and others. See [9,10] again for PS. Below, the borosilicate glass BK7™ and a lithium–aluminium–silicate (LAS) glass ceramic will be added to that list.

Note that these findings are in accordance with the theoretical considerations in [11–13] indicating that the smaller the Prigogine–Defay ratio is for a given glass, the smaller the upper limit for a difference of the volume relaxation kinetics and the enthalpy relaxation kinetics is. ("Small upper limit" means: there may be a difference or there may be none; if there is one, it is small.) PVA and the oxide glass SF64™, for example, have a low Prigogine–Defay ratio (i.e. 2.2 and 1.9, respectively) whereas glassy B_2O_3 has a higher one (i.e. 4.7) [14].

To our knowledge, the derivation of the parameters of the Tool–Narayanaswamy–Moynihan model from DSC measurements and the comparison of the thus characterized enthalpy relaxation kinetics with the volume relaxation kinetics, has been carried out for the first time for an inorganic (lithium aluminium silicate) glass ceramic. See [15] for an earlier oral presentation of part of the glass ceramic data. See [16] for similar results concerning BK7™.

2. The Tool–Narayanaswamy–Moynihan model for the glass transition

To characterize the configurational state of a glass both in the equilibrium and the non-equilibrium state, Tool has introduced the so-called fictive temperature which he has defined as the temperature at which a glass of the given configurational state would be at equilibrium, even if the environmental temperature is different.

During a cooling and reheating cycle, the fictive temperature changes will take the following course. At high temperatures the fictive temperature will be equal to the environmental temperature. In the glass transition range, it will deviate from the environmental temperature and take a constant value when the configurational degrees of freedom are frozen in. This constant value will stay until the glass transition is reached again during reheating. There, it will then start to rise first gradually and then faster. At high temperatures, it will immediately follow the environmental temperature as it did at the beginning of the cycle.

All macroscopic properties which are dependent on the distribution of the atomic ensembles among the possible configurational states, such as enthalpy per mass or thermal expansion, have to be considered as functions of the fictive temperature therefore. A linear relationship which comes on top of the temperature dependence (vibrational part) is assumed:

$$\Delta\text{property} = \chi_{\text{property,vibrational}}\Delta T + \chi_{\text{property,configurational}}\Delta T_\text{f} \quad (2)$$

Together, $\chi_{\text{property, vibrational}}$ and $\chi_{\text{property, configurational}}$ are the generalized susceptibilities such as the specific heat or the thermal expansion coefficient which one finds in the equilibrium state above the glass transition where $T_\text{f} = T$ holds. Below the glass transition, one will find $\chi_{\text{property, vibrational}}$ only. In the glass transition range, one will find a time-dependent response depending on the kinetics of the fictive temperature.

To describe this kinetics, Tool introduced the following differential equation for the fictive temperature [17]:

$$\frac{\mathrm{d}T_\text{f}}{\mathrm{d}t} = \frac{T - T_\text{f}}{\tau} \quad (3)$$

t is the time, and τ is the structural relaxation time constant which depends on the temperature. For the latter, the first guess is an Arrhenius-type law, with τ_0 being a temperature-independent prefactor and H being the (apparent!) activation enthalpy:

$$\tau = \tau_0\,\mathrm{e}^{H/k\cdot T} \quad (4)$$

If a sample with fictive temperature $T_\text{f}(0)$ is exposed to an environment with temperature T and the latter is held constant, then the solution of (3) is a single-exponential function:

$$T_\text{f} = T + (T_\text{f}(0) - T)\,\mathrm{e}^{-t/\tau} \quad (5)$$

Although being suited to describe the essential features of the fictive temperatures, the simple approach represented by (3) and (4) has had to be revised with respect to a number of findings. One observation has been made considering large temperature jumps where the thermal activation has been found to depend on the fictive temperature.

A suited formula taking this into account is an Arrhenius-type thermal activation function depending on both the temperature and the fictive temperature [18,3]:

$$\tau = \tau_0\,\mathrm{e}^{H/k\cdot((x/T)+((1-x)/T_\text{f}))}, \quad 0 < x < 1 \quad (6)$$

x is called nonlinearity parameter for the following reason. If (6) is inserted in (3), the latter will cease to depend linearly on the variable T_f. To make (3) a linear differential equation again, the variable t is replaced by the new variable ζ which is called reduced time [19,20]:

$$\zeta \equiv \int_0^t \frac{\mathrm{d}t'}{\mathrm{e}^{H/k\cdot((x/T(t'))+((1-x)/T_\text{f}(t')))}} \quad (7)$$

Note that (7) differs from the common definition of the reduced time yielding a dimensionless quantity which is equivalent to ζ/τ_0.

Another finding has been on temperature jump experiments carried out at constant temperature T after equilibration at a constant temperature T_0. The kinetics has turned out to be different from a single exponential. For short times, the relaxation is faster than according to a single exponential; for long times, it is slower. Usually a stretched-exponential or Kohlrausch-function fits better:

$$T_\mathrm{f} = T + (T_\mathrm{f}(0) - T)\,\mathrm{e}^{-(\zeta/\tau_0)^b},$$
$$0 < b < 1, \quad T_\mathrm{f}(0) = T_0 \tag{8}$$

b is the so-called Kohlrausch- (who first applied a stretched exponential function on a relaxation process in 1847) or Kohlrausch–Williams–Watts- (the latter two revitalized the stretched exponential function in 1970) parameter [21–23].

Taking these findings into account, one arrives at what is called Tool–Narayanaswamy–Moynihan model today. Below, it will be applied in the following way which covers non-isothermal processes also and is suited for computational purposes:

1. The Kohlrausch-function is represented by a Prony series of single exponentials with coefficients v_i and individual relaxation times $\tau_{0,i}$ allowing for the "fast" and the "slow" part of the Kohlrausch-function. The v_i and $\tau_{0,i}$ are chosen such that an optimum representation of the Kohlrausch-function results. The precision of this representation, of course, depends on the order number n of the Prony series:

$$\mathrm{e}^{-(\zeta/\tau_0)^b} =: \sum_{i=1}^{n} v_i\,\mathrm{e}^{-(\zeta/\tau_{0,i})}, \quad \sum_{i=1}^{n} v_i = 1 \tag{9}$$

2. T_f is represented by a series of $T_{\mathrm{f},i}$. with the coefficients being identical to those of the above Prony series:

$$T_\mathrm{f}(\zeta) =: \sum_{i=1}^{n} v_i \cdot T_{\mathrm{f},i}(\zeta) \tag{10}$$

3. Tool's original differential equation is replaced with a series of differential equations, one for each of the $T_{\mathrm{f},i}$ from above:

$$\frac{\mathrm{d}T_{\mathrm{f},i}}{\mathrm{d}\zeta} = \frac{T - T_{\mathrm{f},i}}{\tau_{0,i}} \tag{11}$$

With the above, the resulting version of the Tool–Narayanaswamy–Moynihan model consists of n differential equations depending on four independent parameters: H, x, τ_0, b. It is consistent with the above findings.

It has to be mentioned that beside the Tool–Narayanaswamy Moynihan (TNM) model there is the Kovacs–Aklonis–Hutchinson–Ramos (KAHR) model, see [24]. Both models have found to be equivalent [25]. In [24], the issue of equal or non-equal relaxation kinetics for enthalpy and volume is explicitly mentioned. It is stated that the formalism applies to both. As for the model parameters, both possibilities of equality and non-equality are considered possible.

Note that the TNM model as applied here, i.e. with one constant apparent thermal activation enthalpy, is valid only over a limited temperature range around the annealing point. For strong glass formers like oxide glasses (or "long" glasses in the nomenclature of the glass makers), this temperature range is broad enough to make it a very powerful tool for most practical cases which is confirmed by the following analysis. It has to be stated that the statement about the correspondence of the time scales for enthalpy and volume found here is limited to this temperature range also. See again [9,10] where volume and enthalpy relaxation are investigated for polystyrene. In the temperature range where the TNM model is applicable, the kinetics found is the same for both processes. Deviations occur when this temperature range is left.

See [26,27] for the evaluation of DSC curves with the TNM model in general. See [28,29] for the application of modulated DSC in this context.

3. Measurement of kinetic processes by differential scanning calorimetry (DSC)

With what has been said above, it is clear that differential scanning calorimetry is well suited to derive the fictive temperature kinetics of any glass, in particular the four parameters of the TNM model. Care must be taken, however, concerning the necessary desmearing or deconvolution of the experimental data. To carry out this, a thorough understanding of the instrument is required.

The principle setup of a heat-flux DSC is this. The sample being investigated is put into a crucible which in return is put into a crucible holder in an oven. In addition to this crucible holder, there is a second crucible holder in the oven with a crucible that is left empty during the measurement and is used as reference. To carry out the measurement, the oven temperature T_O is raised at a constant rate while the sample temperature T_S and, in particular, the difference ΔT between the sample temperature T_S and the reference temperature T_R are being monitored (Fig. 3).

From these data, the heat capacity of a sample can be obtained. Assuming that the heat transfer between oven and sample is proportional to the temperature difference ΔT, divided by a thermal resistance R, and further assuming that the heating rates of the sample, the reference, and the oven are the same, one will arrive at the Tian–Calvet equation in its simplest form. It relates the sample heat capacity C_S to the temperature difference ΔT, the oven heating rate $\mathrm{d}T_\mathrm{O}/\mathrm{dt}$, and the above thermal resistance R [30]:

$$\frac{-\Delta T}{R \cdot \dot{T}_\mathrm{O}} = C_\mathrm{S} \tag{12}$$

The derivation starts at applying some kind of "node rule" at the interface of the crucible mounts and the crucible:

$$\frac{T_\mathrm{O} - T_\mathrm{S}}{R} = (C_\mathrm{C} + C_\mathrm{S}) \cdot \dot{T}_\mathrm{O}, \quad \frac{T_\mathrm{O} - T_\mathrm{R}}{R} = C_\mathrm{C} \cdot \dot{T}_\mathrm{O} \tag{13}$$

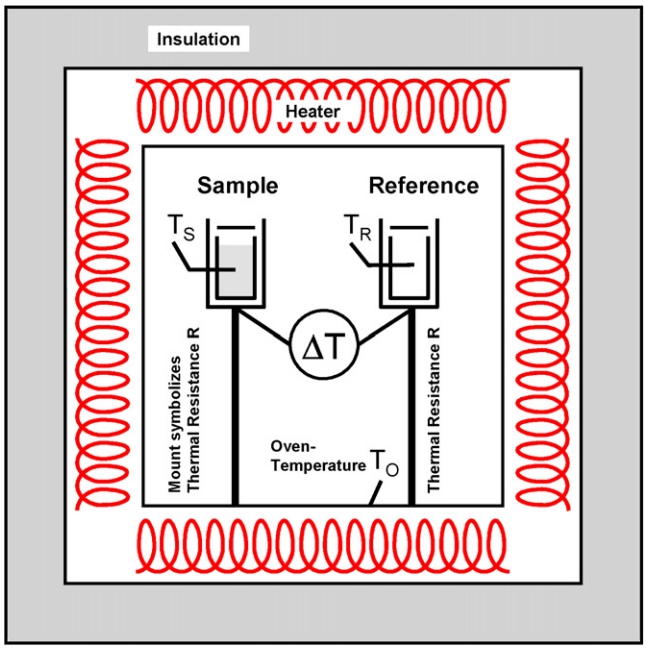

Fig. 3. Principle setup of a heat-flux DSC.

C_C is the heat capacity of the empty crucible. The node rule at the position of the sample crucible holder says that the heat flux coming from the oven, i.e. $(T_O - T_S)/R$ according to the assumption, equals the power required for heating up the sample with its crucible at the oven heating rate, i.e. $(C_C + C_S)\,dT_O/dt$. In a steady state, this node rule obviously applies. For the node rule at the position of the reference crucible, an analogous argument holds.

Combining the two equations of (13), one arrives at (12).

R is obtained from a run on a substance the specific heat of which is known, for instance sapphire (and will turn out to be a weak function of temperature). ΔT is measured, and dT_O/dt is controlled. With this, one may determine the specific heat of any substance via a DSC run, as it has been said above.

However, the above simple version of the Tian–Calvet formalism may not be applied if exothermal or endothermal processes in the sample occur. In that case, the heating rate of the sample may significantly differ from the one of the oven. With the usual setup, this will not even be correctly recorded by the sensor monitoring the sample temperature since the latter is situated on the outer surface of the sample crucible. This has to be allowed for by a DSC model which shall be suited for a correct analysis of the calorimetric glass transition.

There is one type of DSC models starting at a representation of the DSC by an analogon to an electric circuit, with thermal resistances and heat cacities or "*RC*-elements". Depending on the number of *RC*-elements, the models of this type are classified as zeroth-order, first-order, etc. [31].

With such a model and a couple of calibration measurements, the desired structural relaxation data reduction can be carried out in a satisfactory way, as will be shown below (Fig. 4).

According to the extended model considered here, the DSC is represented by three heat capacities and three thermal resistances which are assumed to be separable, i.e. the heat capacities

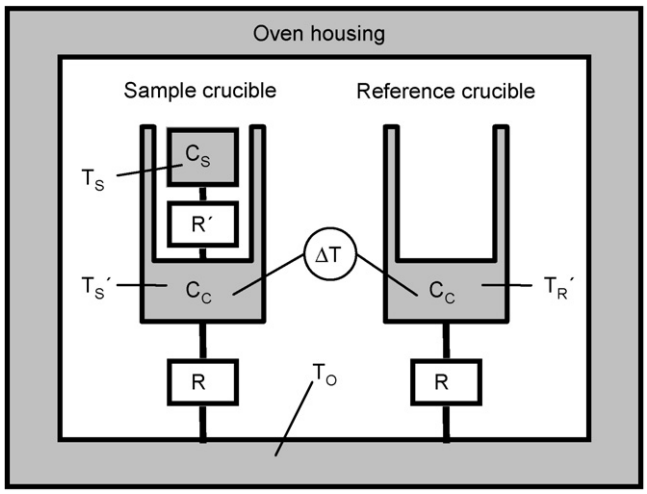

Fig. 4. Representation of a heat-flux DSC by thermal resistances and heat capacities.

have no inherent thermal resistance and vice versa. The empty crucible heat capacity C_C, the sample heat capacity C_S and the thermal resistance R between oven and crucible are the same as above. In order to make the model consistent with the distinction between a sample crucible temperature T_S' (which is assumed to be the one measured by the sensor on the outer surface of the sample crucible) and an actual sample temperature T_S, an additional thermal resistance R' between the sample and the sample crucible is introduced. The reference crucible temperature which is not measured directly is named T_R' here for consistency reasons.

Note that in the presence of exothermic or endothermic processes, C_S should be called "apparent heat capacity" because it comprehends both the heat exchange due to these processes as well as the one due to the real heat capacity.

With this model, the relation between the apparent sample heat capacity C_S and the quantity ΔT measured by the DSC becomes

$$R \cdot C_S \cdot \dot{T}_O + R \cdot C_S \cdot \dot{\Delta T} + R' \cdot C_S \cdot \dot{\Delta T} + R \cdot C_C \cdot \dot{\Delta T} + R \cdot C_C \cdot R' \cdot C_S \cdot \ddot{\Delta T} = -\Delta T \quad (14)$$

One may call (6) "extended Tian–Calvet equation". It is to be classified as second-order with respect to the appearance of the second derivative of ΔT.

The derivation is analogous to the one of the simple version of the Tian–Calvet equation and starts at the following set of equations:

$$\frac{T_O - T_S'}{R} = C_C \cdot \dot{T}_S' + \frac{T_S' - T_S}{R'} \quad \text{(node rule at sample crucible)},$$

$$C_S \cdot \dot{T}_S = \frac{T_S' - T_S}{R'} \quad \text{(node rule at sample)},$$

$$\frac{T_O - T_R'}{R} = C_C \cdot \dot{T}_R' \quad \text{(node rule at reference crucible)}$$

$$\Delta T = T_S' - T_R' \quad \text{(quantity measured by DSC)},$$

$$T_S' \quad \text{(temperature monitored by DSC)} \quad (15)$$

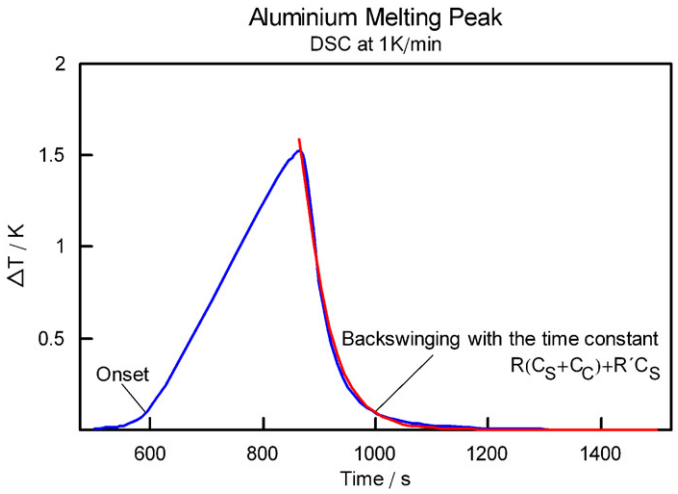

Fig. 5. Determination of the DSC model parameters by evaluation of an aluminium melting peak.

From this set of equation, one may also derive the relation between the actual sample temperature T_S and the measured quantity T'_S:

$$T_S = T'_S + \Delta T \cdot \frac{R'}{R} + \dot{\Delta T} \cdot R' \cdot C_C \tag{16}$$

As it has been said above, R is derived from a calibration measurement on a standard. The additional two parameters that have entered the extended Tian–Calvet equation compared to the simple one can be derived from additional measurements on aluminium (Fig. 5).

Both the ascending and the descending part of the melting peak lead to one equation. At any point of the linearly ascending part, the following equation is valid:

$$\frac{T_O}{R} = C_C \cdot \left(\dot{\Delta T} + \dot{T_O}\right) + \left(\Delta T + T_O - R \cdot C_C \cdot \dot{T'_O}\right) \cdot \times \left(\frac{1}{R'} + \frac{1}{R}\right) - \frac{T_m}{R'} \tag{17}$$

This equation is derived from the following set of equations which is a subset of (15) and is valid as long as the melting of the aluminium goes on

$$\frac{T_O - T'_S}{R} = C_C \cdot \dot{T'_S} + \frac{T'_S - T_m}{R'} \quad \text{(node rule at sample crucible)},$$

$$\frac{T_O - T'_R}{R} = C_C \cdot \dot{T'_O} \quad \text{(node rule at reference crucible)},$$

$$\Delta T = T'_S - T'_R \quad \text{(quantity measured by DSC)} \tag{18}$$

The descending part of the melting peak is described by the extended Tian–Calvet equation which may be simplified in the following way in order to allow an easy evaluation:

$$\begin{aligned} -\Delta T &= R \cdot C_S \cdot \dot{T_O} + R \cdot C_S \cdot \dot{\Delta T} + R' \cdot C_S \cdot \dot{\Delta T} \\ &\quad + R \cdot C_C \cdot \dot{\Delta T} + R \cdot C_C \cdot R' \cdot C_S \cdot \ddot{\Delta T} \approx R \cdot C_S \cdot \dot{T_O} \\ &\quad + R \cdot C_S \cdot \dot{\Delta T} + R' \cdot C_S \cdot \dot{\Delta T} \\ &\quad + R \cdot C_C \cdot \dot{\Delta T} \quad \text{neglecting } \ddot{\Delta T} \Rightarrow \Delta T(t) \\ &= -R \cdot C_S \cdot \dot{T_O} \\ &\quad + \left(\Delta T(0) + R \cdot C_S \cdot \dot{T_O}\right) \mathrm{e}^{-t/(R \cdot (C_S + C_C) + R' \cdot C_S)} \end{aligned} \tag{19}$$

From the simultaneous fit of the Eqs. (17) and (19) to the ascending and the descending part of the aluminium melting peak, C_C and R' are determined (here, C_S is the specific heat of the aluminium sample). With all parameters R, R', and C_C known, an unknown (apparent) C_S can then be determined from (6). For the MHTC96 from Setaram, typical values are $R = 2.4$ K/W, $R' = 3.6$ K/W, and $C_C = 11$ J/K.

The aluminium melting peak is also used for the calibration of the temperature scale. In the limit $dT_O/dt \to 0$, the onset temperature must be equal to the melting point of aluminium [32].

From the temperature and heating rate dependence of C_S, in return, the kinetics of an endothermic or exothermic process can be derived.

4. Application on the glass transition and the dimensional stability issue of glasses

With what has been said in the previous paragraph, the quantity displayed by the DSC measurement of the calorimetric glass transition may be identified as apparent heat capacity or, if referred to the unit mass, apparent specific heat. From these measurements, the derivation of the parameters of the TNM model is possible.

The first step is to evaluate the measurements according to (14). If one compares to an evaluation according to (12), one finds that with the latter one gets a smearing-out of the peak over a broader temperature range, particularly for higher heating rates. So the evaluation according to (14) is equivalent to an desmearing of the otherwise smeared-out curve (Fig. 6).

In the temperature range of a glass transition and above, the enthalpy per time accepted by the sample during heating is partially converted into vibrational enthalpy and partially into configurational enthalpy. The vibrational part of the specific heat and the configurational part of the specific heat are assumed to be constant [4], see above. This means

$$c_{p,\mathrm{apparent}} \cdot \frac{dT_S}{dt} = c_{p,\mathrm{vibrational}} \cdot \frac{dT_S}{dt} + c_{p,\mathrm{configurational}} \cdot \frac{dT_f}{dt} \Rightarrow \frac{dT_f}{dT_S} = \frac{c_{p,\mathrm{apparent}} - c_{p,\mathrm{vibrational}}}{c_{p,\mathrm{configurational}}} \tag{20}$$

Comparing Eq. (20) with the TNM-model from above one finds that the parameters of the latter should be chosen such that the following equation holds approximately:

$$\frac{c_{p,\mathrm{apparent}} - c_{p,\mathrm{vibrational}}}{c_{p,\mathrm{configurational}}} \overset{!}{\approx} \frac{1}{dT_S/dt} \sum_{i=1}^{n} v_i \cdot \frac{T_{f,i}}{dt} \tag{21}$$

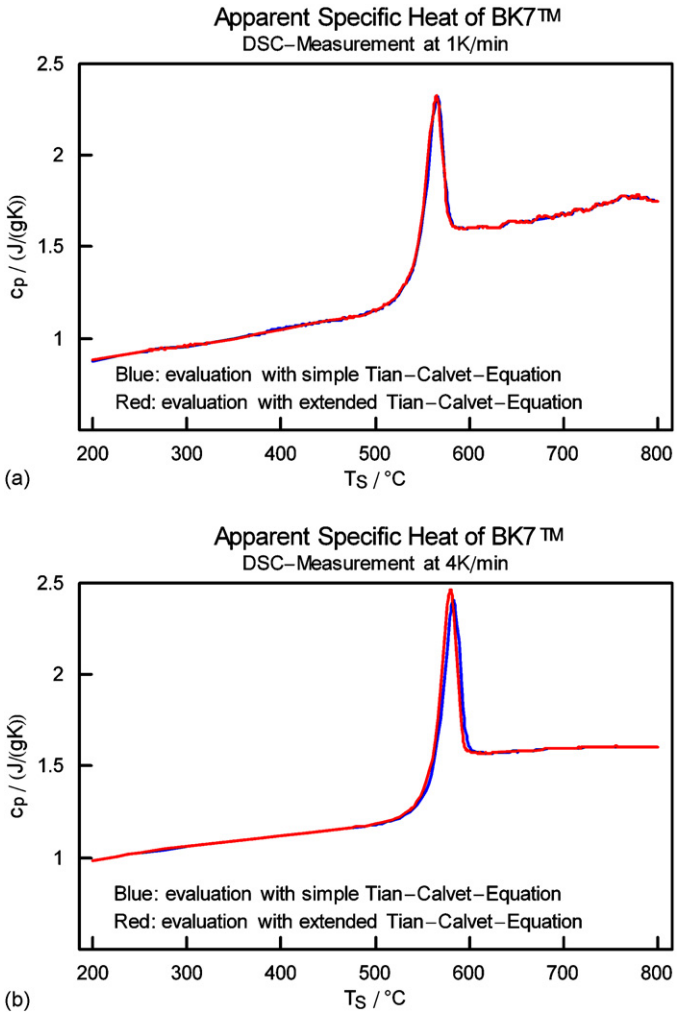

Fig. 6. (a and b) Desmearing of DSC measurements. Without, the centre of the 4 K/min peak would be positioned at a temperature which is too high by 4 K. (For interpretation of the references to color in this figure legend, the reader is referred to the web version of the article.)

This task can be carried out by any fitting routine which is capable of handling differential equations. In each loop, the differential equations (11) are integrated for a given set of TNM model parameters which fitted during the progress of the routine. The initial conditions for the differential equations are obtained the following way. From an integration of (20) starting at a temperature well above the glass transition where $T_f = T$ is valid and over an interval covering the glass transition range, the initial value for the fictive temperature is obtained. At the beginning of each loop of the fitting routine, a linear cooling rate is determined which leads to this initial value of the fictive temperature, now calculated via the TNM model with the given set of TNM model parameters. This calculation gives initial values for the individual $T_{f,i}$ under the assumption that the glass had been exposed to linear cooling before the DSC measurement (which is usually justified).

If one adjusts the parameters subsequently and "by hand", the effect of each parameter on the fit curve will become particularly clear [16]. The resulting fit shows that the Tool–Narayanaswamy Moynihan model allows an almost perfect representation of the measured data. The TNM-model parameters obtained from the DSC for BK7™ are: $\tau_0 = 8.75 \times 10^{-36}$ s, $b = 0.694$, $H/k = 71802.3$ K, $x = 0.695$ (Fig. 7).

Without desmearing, one would get too small a value for the apparent activation enthalpy, approximately by 20%.

These parameters can be used for a prediction of the dimensional stability of a glass sample that is equilibrated at a temperature T_1 first and then exposed to a temperature jump to a temperature T_2. The starting point is the dilatometric equivalent of (20)

$$\frac{dl}{dt} = \alpha_{\text{vibrational}} \cdot \frac{dT}{dt} + \alpha_{\text{configurational}} \cdot \frac{dT_f}{dt} \tag{22}$$

l is the sample length. α stands for the coefficient of thermal expansion.

$\alpha_{\text{vibrational}}$ is usually known from regular thermal expansion measurements. If $\alpha_{\text{configurational}}$ is also known, e.g. from an earlier temperature jump experiment with the sample having been

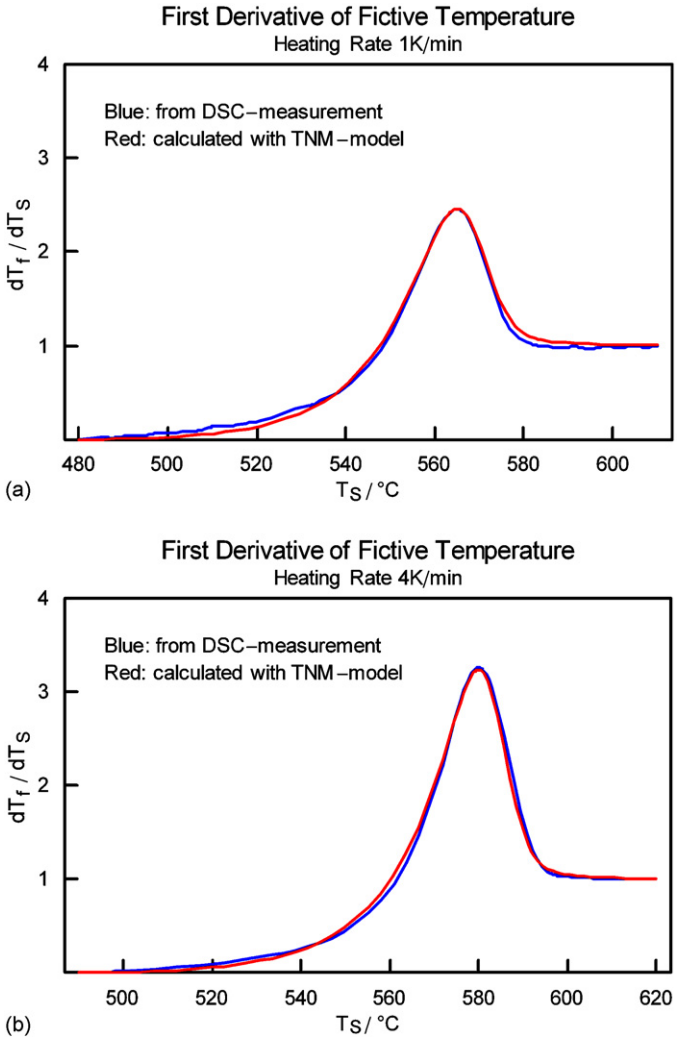

Fig. 7. (a and b) Fit of TNM model to DSC measurements on BK7™. (For interpretation of the references to color in this figure legend, the reader is referred to the web version of the article.)

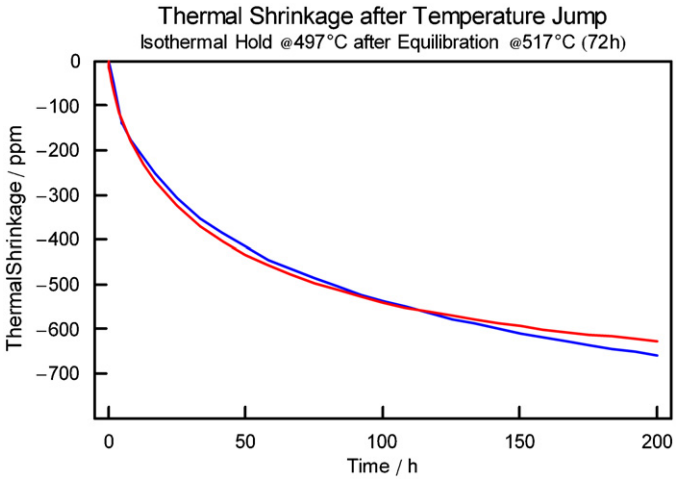

Fig. 8. Compaction prognosis for a temperature jump experiment on BK7^{TM} with the TNM model (H, x, b, τ_0: from DSC, $\alpha_{configurational}$ = 35 ppm/K from density measurement of the melt).

equilibrated both before and after the temperature jump or from a comparison of α in the molten state and $\alpha_{vibrational}$, then the kinetics of the delayed sample shrinkage following the instantaneous vibrational effect can be very satisfactorily predicted for any further temperature jump experiment based on the calculation of $T_f(t)$ by the TNM model with the parameters obtained from a DSC according to the above procedure. Note that without desmearing, the extrapolation of the structural relaxation kinetics from ca. 570 °C, where it is measured, to 510 °C, where the temperature jump experiment takes place, would give a relaxation time at 510 °C which would be wrong by a factor of about 3 (Fig. 8).

One application is the prediction (and tailoring) of the shrinkage of display glasses during the coating processes in flat panel display production.

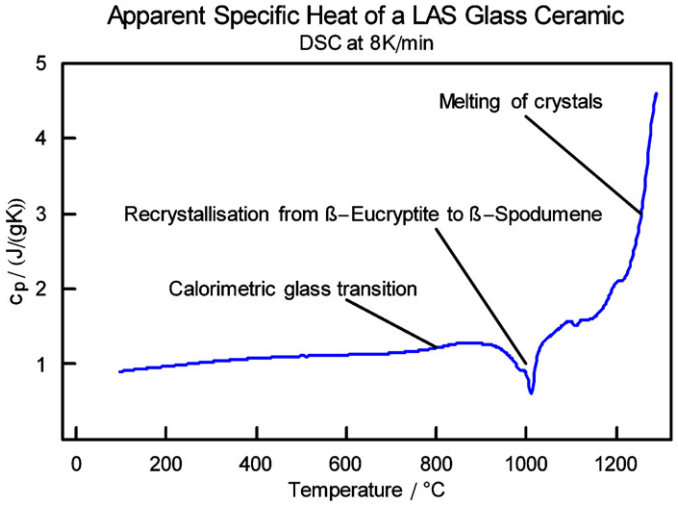

Fig. 9. Apparent specific heat of a lithium–aluminium–silicate (LAS) glass ceramic showing a calorimetric glass transition at ca. 800 °C.

5. Application on the glass transition and the dimensional stability issue of glass ceramics

A calorimetric glass transition can also be found in a glass ceramic (Fig. 9).

This is no surprise since a glass ceramic consists of crystals embedded in a residual glass matrix which should display a glass transition. The small value of the corresponding configurational part of the specific heat of the overall system, i.e. 0.08 J/(g K) compared to 0.3 J/(g K) observed at the borosilicate glass, results from the small share (ca. 30%) which the residual glass phase has in the glass ceramic (for LAS glass ceramics see [33]).

There are two peculiarities of the calorimetric glass transition of a glass ceramic. First, the glass transition occurs at a comparatively high temperature. Second, it is comparatively broad (which corresponds to a small value of the Kohlrausch parameter b). A thorough explanation of these phenomena would require the understanding of structural relaxation under geo-

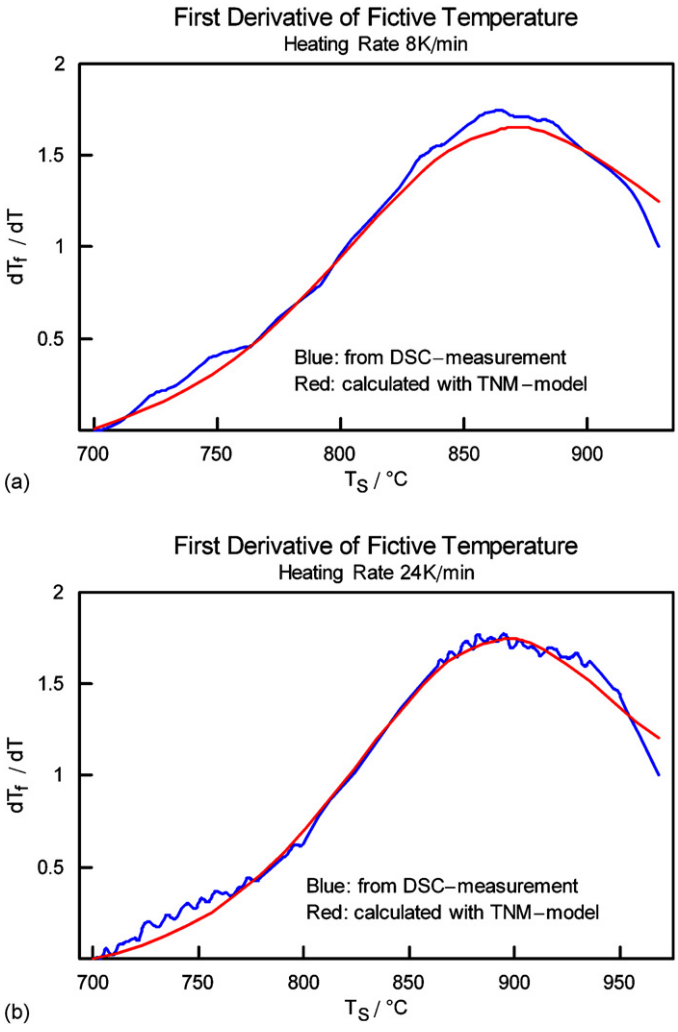

Fig. 10. (a and b) Fit of the TNM model to two DSC measurements of the calorimetric glass transition of a LAS–glass ceramic. (For interpretation of the references to color in this figure legend, the reader is referred to the web version of the article.)

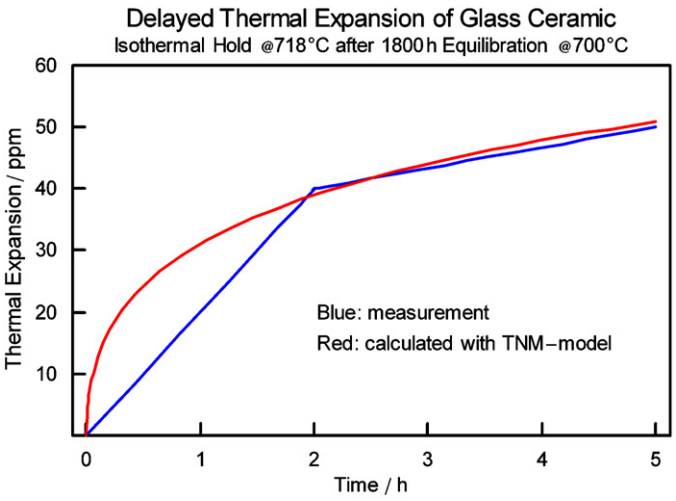

Fig. 11. Temperature up-jump experiment on a LAS–glass ceramic. (For interpretation of the references to color in this figure legend, the reader is referred to the web version of the article.)

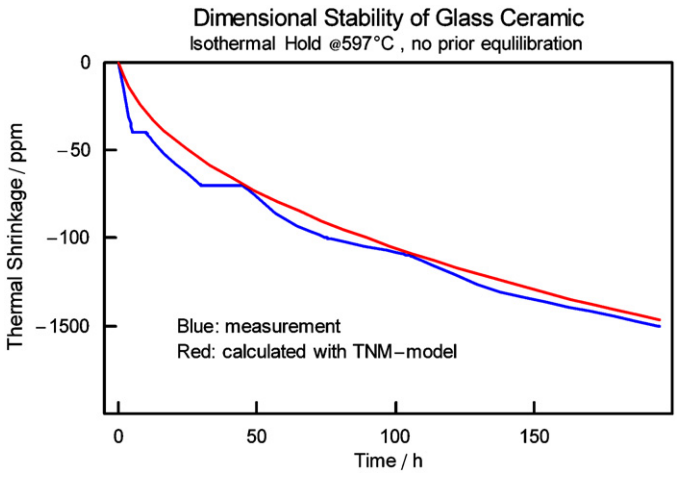

Fig. 12. Dimensional stability prognosis for a LAS–glass ceramic. (For interpretation of the references to color in this figure legend, the reader is referred to the web version of the article.)

metrical constraints, an item that is even more challenging than the understanding of structural relaxation in the bulk (and even the latter does not yet exist in a completely satisfactory way).

However, there are findings that may contribute to an explanation of these observations.

Simulations of a glass film with a dimension which is comparable to the one of the residual glass phase in a typical glass ceramic have shown that in such film, there are two relaxation processes, a fast one with a kinetics similar to the one of the bulk and a slow one which becomes more and more dominant with decreasing film dimension [34]. The slow one is characterized by a small Kohlrausch parameter.

Although the simulated glass has been a theoretical one (a Lennard–Jones glass, with the film being in between walls of frozen glass), one may take this result as one hint that certain geometrical constraints lead to slower relaxation times and, consequently, an increase of the glass transition temperature observed.

Remarkably, the evaluation of the calorimetric glass transition of a glass ceramic with respect to the parameters of the TNM-model allows a prediction of dimensional changes in the same way as for regular glasses (Fig. 10).

The TNM-model parameters obtained from the DSC for the LAS glass ceramic are: $\tau_0 = 9.8 \times 10^{-18}$ s, $b = 0.38$, $H/k = 49{,}076$ K, $x = 1$.

$\alpha_{\text{configurational}}$ is obtained from a temperature up-jump experiment which is simulated by the Tool–Narayanaswamy–Moynihan model with the kinetic parameters as obtained via DSC and $\alpha_{\text{configurational}}$ as only fit parameter. $\alpha_{\text{configurational}} = 5.25$ ppm/K is found (Fig. 11).

Together, all these parameters can be used to predict the outcome of a temperature down-jump experiment. The fact that an up-jump experiment leads to expansion whereas a down-jump experiment leads to shrinkage is another clear hint for the existence of a glass transition since for the latter, depending on thermal history, both shrinkage and dilatation are possible after a temperature jump (Fig. 12).

For a temperature up-jump experiment on a glass ceramic see also [35].

6. Conclusion

Quantitative dimensional stability predictions can be made with the Tool–Narayanaswamy–Moynihan model and DSC-derived model parameters both for the borosilicate glass BK7^{TM} and an LAS glass ceramic in the respective glass transition ranges. The appropriate deconvolution of the DSC curves is a precondition.

References

[1] G. Adam, J.H. Gibbs, On the temperature dependence of cooperative relaxation properties in glass-forming liquids, J. Chem. Phys. 43 (1965) 139–146.
[2] E.-J. Donth, Relaxation and Thermodynamics in Polymers, Akademie-Verlag, Berlin, 1992, pp. 187–191.
[3] C.T. Moynihan, A.J. Easteal, M. Ann DeBolt, J. Tucker, Dependence of the fictive temperature of glass on cooling rate, J. Am. Ceram. Soc. 59 (1976) 12–16.
[4] G.W. Scherer, Relaxation in Glass and Composites, Krieger Publishing Company, Malabar, 1992, pp. 113–174.
[5] M. Ann DeBolt, A.J. Easteal, P.B. Macedo, C.T. Moynihan, Analysis of structural relaxation in glass using rate heating data, J. Am. Ceram. Soc. 59 (1–2) (1976) 16–21.
[6] S.L. Simon, D.J. Plazek, J.W. Sobieski, E.T. McGregor, Physical aging of a polyetherimide: volume recovery and its comparison to creep and enthalpy measurements, J. Polym. Sci., Part B: Polym. Phys. 35 (6) (1997) 929–936.
[7] G. Joachim, D. Donald, G. Conrad, Thermal expansion of silicate liquids: direct determination using container-based dilatometry, Am. Mineral. 84 (1999) 1176–1180.
[8] J. Marek, Volume and enthalpy relaxation in glassy materials, Macromolecules 31 (1998) 8312–8322.
[9] S.L. Simon, J.W. Sobieski, D.J. Plazek, Volume and enthalpy recovery of polystyrene, Polymer 42 (6) (2001) 2555–2567.
[10] P. Badrinarayanana, S.L. Simon, Origin of the divergence of the timescales for volume and enthalpy recovery, Polymer 48 (6) (2007) 1464–1470.

[11] C.T. Moynihan, P.K. Gupta, Order parameter model for structural relaxation in glass, J. NonCryst. Sol. 29 (2) (1978) 143–158.
[12] J.I. Berg, A.R. Cooper, Linear non-equilibrium thermodynamic theory of glass-transition kinetics, J. Chem. Phys. 68 (10) (1978) 4481–4485.
[13] A.V. Lesikar, C.T. Moynihan, Some relations connecting volume and enthalpy relaxation in the order parameter model of liquids and glasses, J. Chem. Phys. 72 (12) (1980) 6422–6423.
[14] C.T. Moynihan, A.V. Lesikar, Comparison and analysis of relaxation processes at the glass transition temperature, Ann. N. Y. Acad. Sci. 371 (1981) 151–169.
[15] U. Fotheringham, K. Erb, A. Baltes, E. Weiß, R. Dudek, F. Siebers, Zum kalorimetrischen Glasübergang von Glaskeramiken. Presentation at "79. Glastechnische Tagung", Würzburg, May 23–25, 2005, No. S2-1610 on Abstract-CD, 2001.
[16] U. Fotheringham, Applying the dynamics of the structure to tailor the glass properties, in: Analysis of the Composition and Structure of Glass and Glass Ceramics (Schott Series on Glass and Glass Ceramics), Springer-Verlag, Berlin, 1999, pp. 313–343.
[17] A.Q. Tool, J.B. Saunders, Expansion effects of annealing borosilicate thermometer glasses, J. Res. Natl. Bur. Stand. 34 (1945) 199–211.
[18] O.S. Narayanaswamy, A model of structural relaxation in glass, J. Am. Ceram. Soc. 54 (1971) 491.
[19] I.L. Hopkins, Stress relaxation or creep of linear viscoelastic substances under varying temperature, J. Polym. Sci. 28 (1958) 631–633.
[20] R. Gardon, O.S. Narayanaswamy, Stress and volume relaxation in annealing flat glass, J. Am. Ceram. Soc. 53 (1970) 380–385.
[21] R. Kohlrausch, Nachtrag uber die Elastische Nachwirkung beim Cocon- und Glasfaden, und die Hygroskopische Eigenschaft des Ersteren, Pogg. Ann. 72 (1847) 393–425.
[22] G. Williams, D.C. Watts, Non-symmetrical dielectric relaxation behavior arising from a simple empirical decay function, Trans. Faraday Soc. (1970) 80–85.
[23] O. Mazurin, Relaxation phenomena in glass, J. Non-Cryst. Sol. 25 (1977) 130–169.
[24] A.J. Kovacs, J.J. Aklonis, J.M. Hutchinson, A.R. Ramos, Isobaric volume and enthalpy recovery of glasses. II. A transparent multiparameter theory, J. Polym. Sci.: Polym. Phys. Ed. 17 (1979) 1097–1162.
[25] I.M. Hodge, Adam–Gibbs formulation of enthalpy relaxation near the glass transition, J. Res. Natl. Inst. Stand. Technol. 102 (1997) 195–205.
[26] J.M. O'Reilly, I.M. Hodge, Effects of heating rate on enthalpy recovery in polystyrene, J. Noncryst. Sol. 131 (1991) 451–456.
[27] A.J. Pappin, J.M. Hutchinson, M.D. Ingram, Enthalpy relaxation in polymer glasses—evaluation and interpretation of the Tool–Naryanaswamy–Moynihan parameter x for polyvinylchloride, Macromolecules 25 (3) (1992) 1084–1089.
[28] J. Schawe, A description of the glass transition measured by temperature modulated differential scanning calorimetry, Colloid Polym. Sci. 276 (7) (1998) 565–569.
[29] C. Schick, M. Merzlyakov, A. Hensel, Nonlinear thermal response at the glass transition, J. Chem. Phys. 111 (6) (1999) 2695–2700.
[30] G. Höhne, W. Hemminger, H.-J. Flammersheim, Differential Scanning Calorimetry, Springer Verlag, Berlin, 1996, pp. 21–24.
[31] G. Höhne, W. Hemminger, H.-J. Flammersheim, Differential Scanning Calorimetry, Springer Verlag, Berlin, 1996, pp. 28–33.
[32] G. Höhne, W. Hemminger, H.-J. Flammersheim, Differential Scanning Calorimetry, Springer Verlag, Berlin, 1996, pp. 43–61.
[33] W. Pannhorst, Glass ceramics based on lithium aluminium silicate solid solution crystals, in: Low Thermal Expansion Glass Ceramics (Schott Series on Glass and Glass Ceramics), Springer-Verlag, Berlin, 1995, pp. 39–46.
[34] P. Scheidler, W. Kob, K. Binder, The relaxation dynamics of a supercooled liquid confined by rough walls, J. Phys. Chem. B 108 (2004) 6673–6694.
[35] A. Sakamoto, S. Fujita, S. Yamamoto, Long-term dimensional stability of glass ceramics, in: XX International Congress on Glass, Kyoto, September 28, 2004.